

SANDIA REPORT

SAND2016-0837

Unlimited Release

Printed February, 2016

Helium trapping at erbium oxide precipitates in erbium hydride

Stephen M. Foiles, Corbett C. Battaile

Prepared by

Sandia National Laboratories

Albuquerque, New Mexico 87185 and Livermore, California 94550

Sandia National Laboratories is a multi-program laboratory managed and operated by Sandia Corporation, a wholly owned subsidiary of Lockheed Martin Corporation, for the U.S. Department of Energy's National Nuclear Security Administration under contract DE-AC04-94AL85000.

Approved for public release; further dissemination unlimited.



Sandia National Laboratories

Issued by Sandia National Laboratories, operated for the United States Department of Energy by Sandia Corporation.

NOTICE: This report was prepared as an account of work sponsored by an agency of the United States Government. Neither the United States Government, nor any agency thereof, nor any of their employees, nor any of their contractors, subcontractors, or their employees, make any warranty, express or implied, or assume any legal liability or responsibility for the accuracy, completeness, or usefulness of any information, apparatus, product, or process disclosed, or represent that its use would not infringe privately owned rights. Reference herein to any specific commercial product, process, or service by trade name, trademark, manufacturer, or otherwise, does not necessarily constitute or imply its endorsement, recommendation, or favoring by the United States Government, any agency thereof, or any of their contractors or subcontractors. The views and opinions expressed herein do not necessarily state or reflect those of the United States Government, any agency thereof, or any of their contractors.

Printed in the United States of America. This report has been reproduced directly from the best available copy.

Available to DOE and DOE contractors from
U.S. Department of Energy
Office of Scientific and Technical Information
P.O. Box 62
Oak Ridge, TN 37831

Telephone: (865) 576-8401
Facsimile: (865) 576-5728
E-Mail: reports@adonis.osti.gov
Online ordering: <http://www.osti.gov/bridge>

Available to the public from
U.S. Department of Commerce
National Technical Information Service
5285 Port Royal Rd
Springfield, VA 22161

Telephone: (800) 553-6847
Facsimile: (703) 605-6900
E-Mail: orders@ntis.fedworld.gov
Online ordering: <http://www.ntis.gov/help/ordermethods.asp?loc=7-4-0#online>



Helium trapping at erbium oxide precipitates in erbium hydride

Stephen M. Foiles and Corbett C. Battaile
Computational Materials and Data Science Department
Sandia National Laboratories
Albuquerque, NM 87185

Abstract

The formation of He bubbles in erbium tritides is a significant process in the aging of these materials. Due to the long-standing uncertainty about the initial nucleation process of these bubbles, there is interest in mechanisms that can lead to the localization of He in erbium hydrides. Previous work has been unable to identify nucleation sites in homogeneous erbium hydride. This work builds on the experimental observation that erbium hydrides have nano-scale erbium oxide precipitates due to the high thermodynamic stability of erbium oxide and the ubiquitous presence of oxygen during materials processing. Fundamental DFT calculations indicate that the He is energetically favored in the oxide relative to the bulk hydride. Activation energies for the motion of He in the oxide and at the oxide-hydride interface indicate that trapping is kinetically feasible. A simple kinetic Monte Carlo model is developed that demonstrates the degree of trapping of He as a function of temperature and oxide fraction.

Acknowledgment

This work benefits from extensive prior computational and experimental work on the behavior of Helium in Erbium Hydride and oxide precipitation by Dwight Jennison, Peter Schultz, Clark Snow, Ryan Wixom, Chad Parish and Luke Brewer.

Contents

Nomenclature	8
1 Introduction	9
2 He in Erbium Hydride	11
3 He in Erbium Oxide	13
4 He diffusion barriers	19
5 Kinetic Models	23
6 Summary	25
References	26
Appendix	
A DFT Calculations	29

List of Figures

2.1	Erbium-Hydrogen phase diagram	12
3.1	The cubic bixbyite structure of Er_2O_3 unit cell. The cell is composed of eight units each of which is approximately a cubic face-centered-cubic cell of Er atoms with 6 O atoms located in tetrahedral sites in each cell. Each cell also contains two vacant tetrahedral sites that are located along body diagonals. .	14
3.2	The calculated excess energy associated with adding He atoms to erbium oxide for constant pressure (diamonds) and constant hydride lattice constant (squares) plotted as a function of the concentration of He atoms relative to the number of vacant tetrahedral sites in the oxide. For concentrations less than or equal to one, the heliums are located in T sites and for higher concentrations the additional heliums are located in O_1 sites.	17
4.1	The energy as a function of the reaction coordinate for the motion of the He atom from the T site to the a) O_1 site and to the b) O_2 site.	21
4.2	The energy along the He transition path from an octahedral site in the hydride adjacent to the oxide through an octahedral site in the interface plane, reaction coordinate = 0.5, to a vacant tetrahedral site in the oxide.	22
5.1	The percent of the total simulation time that the diffusing helium atom spends in the oxide phase, as a function of temperature, for several oxide volume fractions.	24

List of Tables

3.1	Locations of the tetrahedral, T, sites in units of $(a/4)$ where a is the lattice constant of the quasi-FCC unit cell (i.e. half the oxide lattice constant) divided into four classes based on the orientation the the respective T site rows.	15
3.2	Computed energy of a He atom at the tetrahedral, T, and two distinct octahedral sites, O_1 and O_2 .	15
5.1	Energy barriers for helium diffusion between the hydride and oxide phases of erbium. Multiple values indicate more than one viable diffusion path for that case, for which the associated diffusion rates - see Equ 5.1 - are summed.	24

Nomenclature

Er Erbium

H Hydrogen

He Helium

O Oxygen

FCC Face-Centered-Cubic

DFT Density Functional Theory based electronic structure calculations

VASP Vienna Ab Initio Simulation Package

NEB Nudged Elastic Band

kMC kinetic Monte Carlo

Chapter 1

Introduction

Helium incorporated into a metal or metal hydride either via implantation or radioactive decay of tritium is in an energetically unstable state. There is a strong energetic preference for the He atom to either leave the metal or trap at defect sites which are more energetically favorable than the bulk lattice. Thus a fundamental challenge concerning the behavior of He incorporated in metal hydrides in general and erbium hydride in particular is the identification of trap sites that can localize significant amounts of He. Such trapping sites may be related to the nucleation of He bubbles which is observed to occur at significant He concentrations. Experimental results on the growth of He bubbles in erbium tritide have been recently reviewed by Snow, et al [13]. In this report, electronic density functional theory (DFT) calculations using the Vienna Ab Initio Simulation Package (VASP) will be used to explore the energetics of one possible trap site for He, namely oxide precipitates. The results indicate that such precipitates can act as strong trapping sites for He in erbium hydride.

For the case of He in erbium hydride, DFT calculations have been performed by Wixom et al [14]. In that study, the detailed migration mechanisms for He in the bulk hydride lattice were addressed. In addition, the energetics of He interactions with various defects in the arrangement of the hydrogen atoms was examined. In this report, the energetics of the He in various potential lattice sites in and near oxide precipitates will be presented and the barriers to the diffusion of the He in and near the oxide precipitates are computed. These results are incorporated into a kinetic Monte Carlo (kMC) analysis of the trapping of He at the oxide precipitates.

The energetics are calculated in this report using electronic density function theory which implements an approximate solution of the quantum mechanical equations for the behaviors of the electrons in order to determine the energetics of the various defect configurations and transition paths. The details of the DFT calculations using VASP are presented in the Appendix.

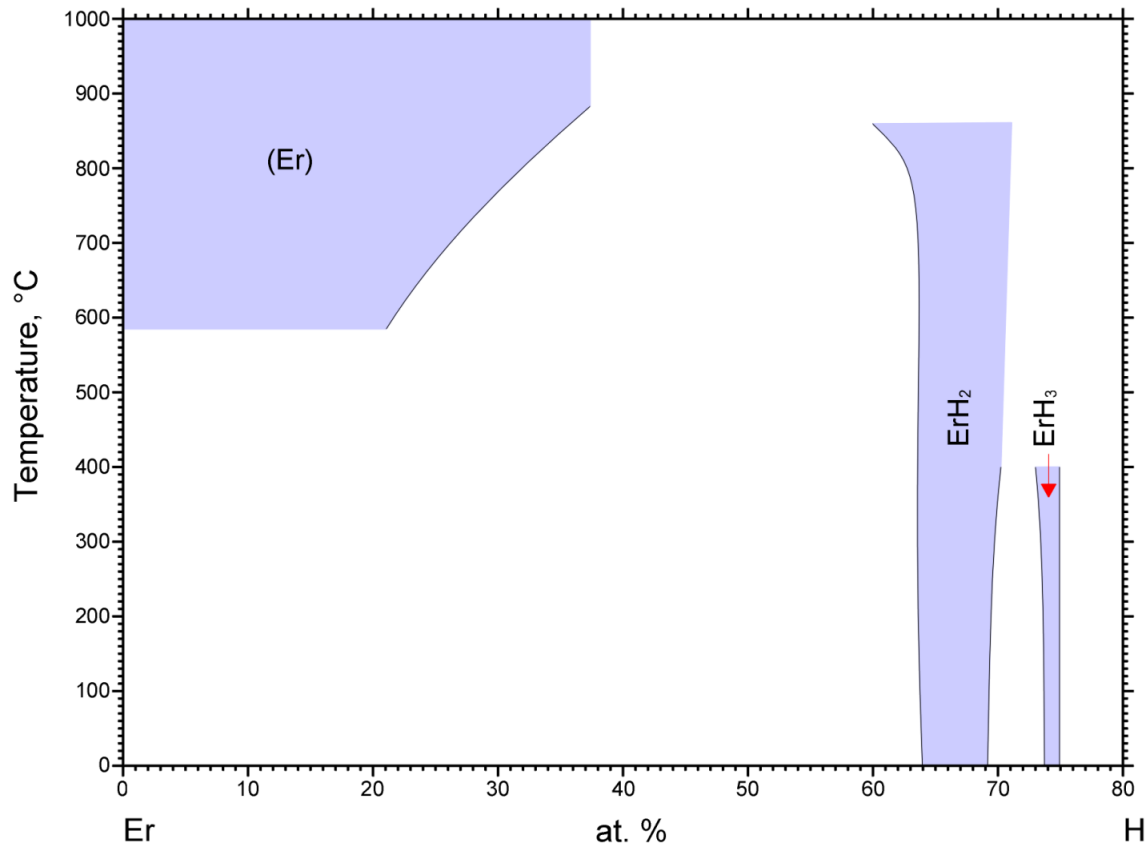
Chapter 2

He in Erbium Hydride

While the focus of this report is on the role of oxide precipitates, it is first necessary to establish the basic energetics of He in the surrounding hydride. For an ideal stoichiometric ErH_2 solid, the Er atoms sit on the sites of a face-centered-cubic (FCC) lattice and the hydrogen atoms are located at the tetrahedral interstitial sites of the FCC lattice. The obvious location for the He atom is in the octahedral site of the Er lattice. The computed energy of the He atom in this site is 1.64 eV. In this context, the He atom energy is taken relative to the energy of the stoichiometric hydride and a free He atom. Note that this energy indicates that the He atom in the bulk hydride is at a higher energy state than the free atom and so has a strong energetic driving force to leave the system. The helium will in practice, though, largely remain in the lattice. This is indicative of the many traps in the lattice that prevent its diffusion out of the sample.

It is important to note that the erbium hydride phase exists over a range of hydrogen concentrations as shown by the phase diagram [10] in Figure 2.1. Excess hydrogen resides in the octahedral sites, while in the sub-stoichiometric case, the hydrogen deficiency is accommodated by the formation of hydrogen vacancies in the tetrahedral site. This indicates the potential importance of defects in the hydrogen arrangement.

The interaction energy of He with dilute hydrogen vacancies is computed as follows. First, the energy and relaxed structure of the hydrogen vacancy is obtained. Next, a He atom is added either in the octahedral site adjacent to the H vacancy or in the empty tetrahedral site. The resulting energy difference yields the He atom energy in the vicinity of the H vacancy. For He in the octahedral site adjacent to the vacancy, the energy is 1.62 eV, which is a minor reduction from the octahedral site energy in the ideal bulk. In contrast, He is strongly bound to the H vacancy with an energy of 1.15 eV. Thus the He atom will bind to any H vacancies with a binding energy of 0.49 eV. This is a substantial trap energy. This indicates that the thermodynamics and kinetics of He in the hydride will require a treatment that considers both the He and its interactions with hydrogen vacancies. Various energies and diffusion barriers associated with the system of He and H vacancies have been determined by Wixom et al [14]. For this report, it is important to remember the energy of 1.15 eV for the energy of He in a hydrogen vacancy site in the hydride since this is likely the energy of dilute He in the hydride lattice.



© ASM International 2006. Diagram No. 900960

Figure 2.1. Erbium-Hydrogen phase diagram

Chapter 3

He in Erbium Oxide

Parish, Snow and Brewer [12] observed small oxide particles in erbium hydrides, presumably due to the high thermodynamic stability of erbium oxide and the ubiquitous presence of oxygen impurities in processing environments. Diffraction experiments indicate that the oxides are coherent with the hydride matrix. The bixbyite structure of the sesquioxide Er_2O_3 is shown in Figure 3.1 from Mao, et al [9].

This structure can be qualitatively described as an FCC erbium lattice with oxygen atoms occupying three fourths of the tetrahedral sites. The remaining vacant tetrahedral sites are arranged in lines along the four different $\langle 1\ 1\ 1 \rangle$ directions of the erbium lattice. The measured lattice constant of this structure is 1.0543 nm [2]. There are two important features of this structure. First, the structure contains a large number of vacant tetrahedral sites in the erbium lattice. In the case of erbium hydride, the vacant tetrahedral sites are energetically favorable sites for the presence of He, which suggests that the vacant tetrahedral sites in the oxide may also be favorable for occupation by He. Second, the lattice constant is close to twice that of erbium hydride. The cubic lattice constant for erbium hydride is 0.5129 nm so the lattice constant of erbium oxide is only 2.8% greater than twice the hydride lattice constant. Since the oxide structure has Er atoms arranged in an approximately FCC manner, this suggests that the oxide will form coherent precipitates in the hydride consistent with the experimental observation.

As a first step, the energetics of He in bulk Er_2O_3 will be determined. The Er atoms are approximately located on the sites of a face-centered-cubic (FCC) lattice. For an FCC lattice, there are two types of interstitial sites, octahedral and tetrahedral. In a cubic cell of the FCC lattice there are eight tetrahedral sites located at $(a/4)(1, 1, 1)$ and four octahedral sites located at $(a/2)(1, 1, 1)$, $(a/2)(1, 0, 0)$, $(a/2)(0, 1, 0)$, and $(a/2)(0, 0, 1)$ where a is the lattice constant. In the bixbyite structure, oxygen atoms occupy six of the tetrahedral sites in each FCC-like cell. The two vacant tetrahedral sites are located along a cube diagonal. The bixbyite structure can be viewed as eight FCC cells each with two vacant tetrahedral sites along the cube diagonal. The cells are arranged and the cube diagonals oriented such that there are periodic chains of vacant tetrahedral sites along the four $\langle 1\ 1\ 1 \rangle$ directions. Due to the incomplete occupation of the tetrahedral sites of the FCC lattice, the Er atom positions are distorted from their ideal FCC locations. The nature of this distortion allows for shorter Er-O bonds. There are three logical locations for a He atom in this lattice. One class of sites is the vacant tetrahedral sites. In the following, these sites will be as denoted as

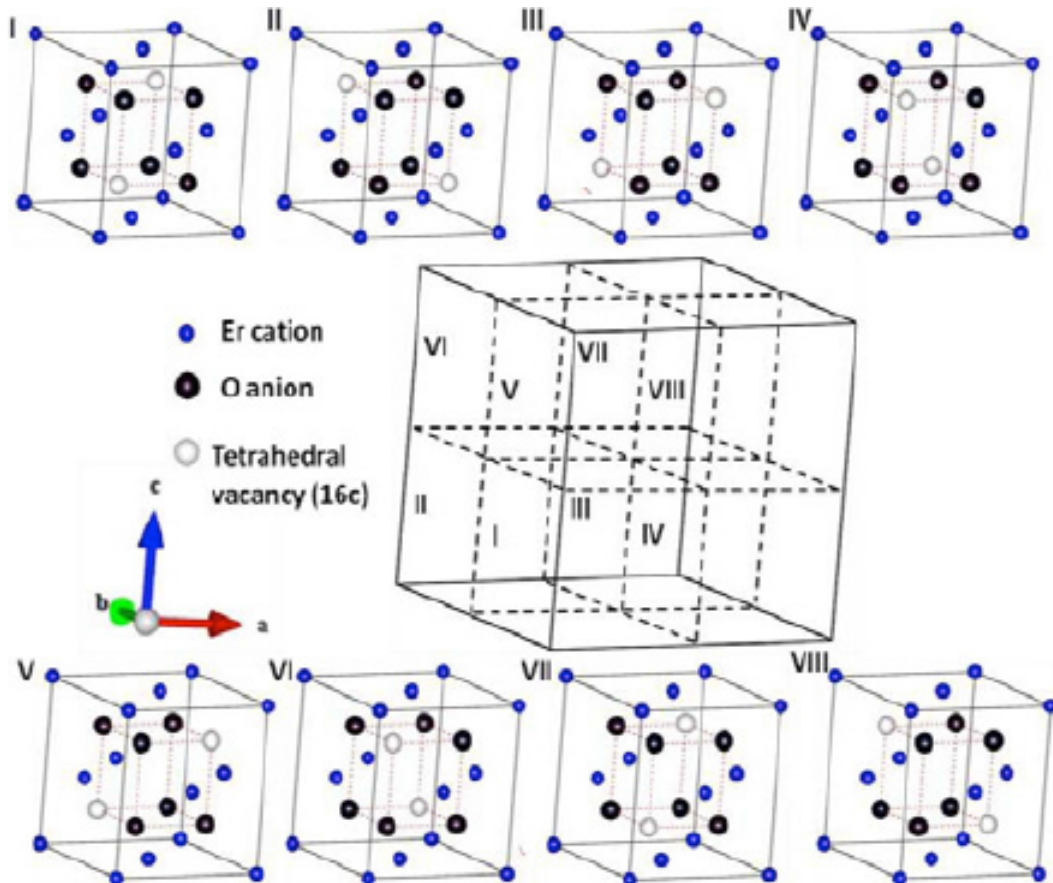


Figure 3.1. The cubic bixbyite structure of Er_2O_3 unit cell. The cell is composed of eight units each of which is approximately a cubic face-centered-cubic cell of Er atoms with 6 O atoms located in tetrahedral sites in each cell. Each cell also contains two vacant tetrahedral sites that are located along body diagonals.

T. The other logical locations for the He are the octahedral interstices of the Er lattice. Due to the partial occupation by oxygen of the tetrahedral interstices, there are two symmetry-inequivalent octahedral sites. The first is the octahedral site at the cube center that is located between two T sites. This site will be denoted O_1 . The other octahedral sites are located on the cube edges. There are three such sites in each FCC cube and they will be denoted here as O_2 .

The locations of the T sites in the bixbyite structure can be grouped into four classes depending on the orientation of the row of T sites. The four classes of T sites will be denoted as A, B, C, and D. The locations of these sites are described in Table 3.1 in units of $(a/4)$ where a is the lattice constant of the quasi-fcc unit cell (4 Er atoms). Note that these sites repeat periodically in all three directions with a period of 8.

Table 3.1. Locations of the tetrahedral, T, sites in units of $(a/4)$ where a is the lattice constant of the quasi-FCC unit cell (i.e. half the oxide lattice constant) divided into four classes based on the orientation the the respective T site rows.

T_A	[1 1 1] row direction	(1,1,1)	(3,3,3)	(5,5,5)	(7,7,7)
T_B	[-1 1 1] row direction	(1,7,3)	(3,5,1)	(5,3,7)	(7,1,5)
T_C	[1 -1 1] row direction	(1,3,5)	(3,1,7)	(5,7,1)	(7,5,3)
T_D	[1 1 -1] row direction	(1,5,7)	(3,7,5)	(5,1,3)	(7,3,1)

The computed energy of a He atom at each of these sites is shown in Table 3.2. Note that these energies are computed at the (constant) equilibrium volume of the oxide and are relative to the free He atom. The preferred location is the T site with the O_1 site being 0.15 eV higher in energy and the O_2 site 0.45 eV higher. Further note that the energy of the He atom in both the T site and the O_1 site is below that of the energy of a He atom in a vacant hydrogen site of the bulk hydride lattice. Thus they are possible trapping sites.

Table 3.2. Computed energy of a He atom at the tetrahedral, T, and two distinct octahedral sites, O_1 and O_2 .

Site	Energy (eV)
T	0.80
O_1	0.95
O_2	1.25

The underlying physical origin of the preference of the He to sit in the vacant tetrahedral sites of the oxide compared to a vacant tetrahedral site (hydrogen vacancy) in the hydride can be understood in terms of the geometry of Er_2O_3 . While the erbium positions form an approximately FCC lattice, they are in fact displaced from the ideal FCC sites due to the presence of O atoms in only three fourths of the tetrahedral sites. Further, the strong Er-O bond pulls the Er atoms towards the O atoms. This has the effect of opening up the vacant

tetrahedral sites. To make this more quantitative, consider the distance from the center of the tetrahedral site to the surrounding Er atoms. This distance is 0.222 nm for the hydride and 0.245 nm for the vacant tetrahedral sites of the oxide. Since the interaction of the He with the surrounding metal atoms is repulsive, this geometric argument is consistent with the predictions of the DFT calculations.

This result suggests that He may bind to oxide precipitates. There are a couple of important questions to be answered, though. First, the above calculation is performed for the bulk oxide under zero external pressure. In reality, the oxide precipitate is embedded in the hydride phase that has a somewhat smaller lattice constant. As a result, the oxide precipitate will be under compression. This is anticipated to increase the He interstitial energy in the precipitate. The He interstitial energy quoted above is expected to be a lower bound on the energy of the He interstitial in the oxide precipitate. An upper bound on the He energy in the precipitate can be obtained by assuming that the lattice constant of the oxide is fixed at the value of the hydride phase. Since the oxide is stiffer than the hydride matrix, this will overestimate the compression of the oxide due to the hydride matrix and so the resulting He interstitial energy will be an upper bound. Calculations of the He interstitial in pure erbium oxide performed at the hydride lattice constant yield a He interstitial energy in the vacant tetrahedral, T, site of 0.98 eV. This is still below the energy of the He in a hydrogen vacancy in the hydride.

A second question is whether there is a strong He-He repulsion between interstitials residing in nearby sites of the oxide. Such repulsion would limit the amount of He that the oxide would trap. To address this question, the energy of varying numbers of He atoms in an oxide unit cell was computed. These computations were performed with two different boundary conditions, zero pressure and constant hydride phase lattice constant. These two calculations will again correspond to lower and upper bounds on the energy of the He interstitials. The energy of the oxide with the He interstitials relative to the energy of the oxide is plotted in Figure 3.2 as a function of the fraction of the vacant tetrahedral sites. For He concentrations greater than one, the extra He atoms are located in octahedral sites of the oxide lattice.

There are various important observations from the data in Figure 3.2. The slopes of the curves reflect the energy required to add an additional He. For both limits, the energy is essentially linear up to a concentration of 1. This indicates that there is only minimal interaction between the He. Thus it should be possible for all of the vacant tetrahedral sites to trap He. For concentrations greater than 1, the slope increases since the additional He atoms now occupy the less favorable octahedral sites. For the lower bound (constant pressure) the slope suggests that the occupation of some of the octahedral sites is still favorable relative to the energy of the He in a vacant hydrogen site in the hydride. For the upper bound (constant hydride lattice constant) the slope above 1 indicates that additional He have an energy of about 1.2 eV which is above the energy for He in the vacant hydrogen site of the hydride. These results indicate that the oxide can at least trap one He for each vacant tetrahedral site and possibly some additional He in the octahedral sites. The question of additional trapping to the octahedral sites will require a more complete treatment of the state of strain of the

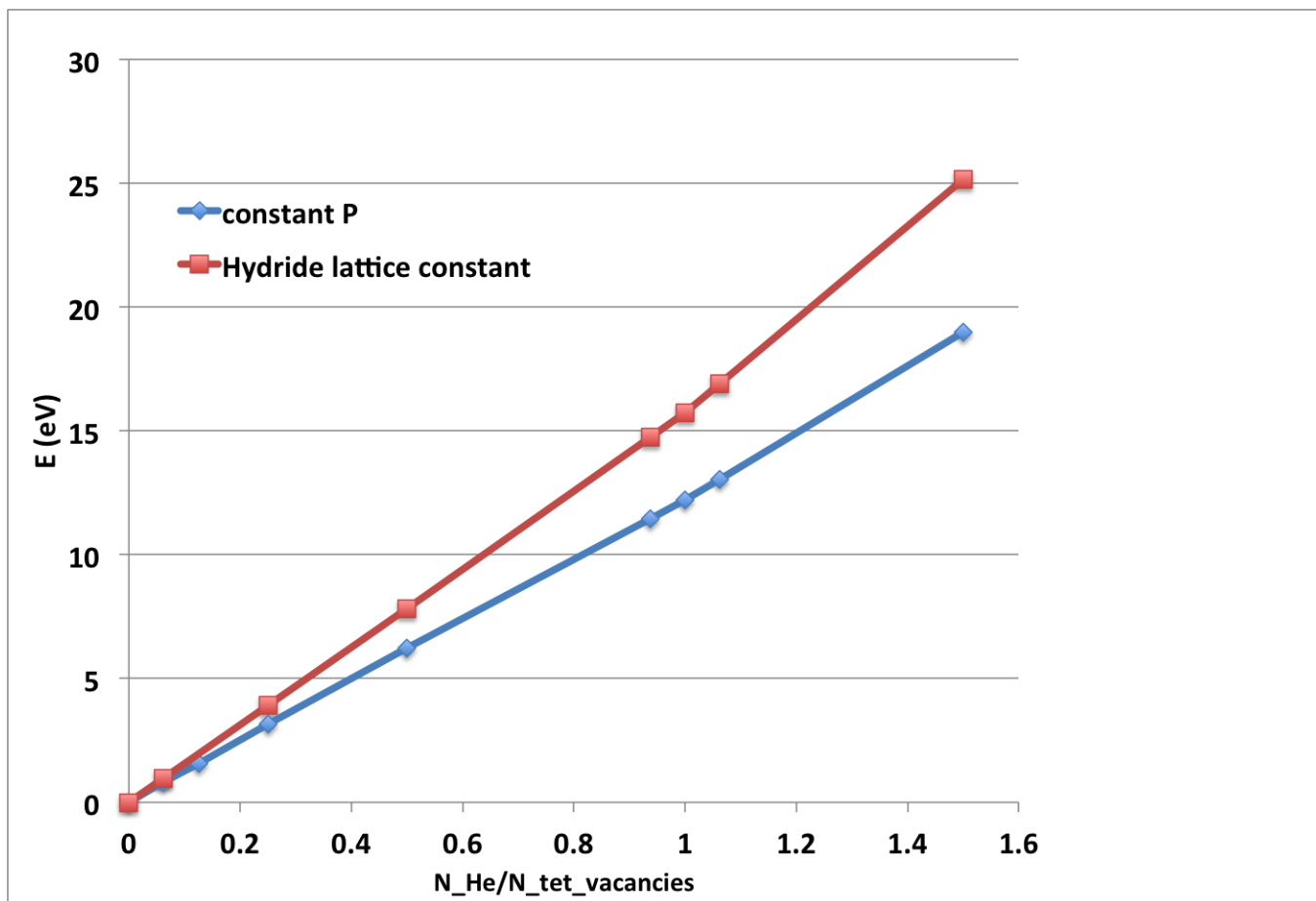


Figure 3.2. The calculated excess energy associated with adding He atoms to erbium oxide for constant pressure (diamonds) and constant hydride lattice constant (squares) plotted as a function of the concentration of He atoms relative to the number of vacant tetrahedral sites in the oxide. For concentrations less than or equal to one, the heliums are located in T sites and for higher concentrations the additional heliums are located in O_1 sites.

oxide precipitates.

As a first step towards understanding the stress state in an oxide precipitate, a model precipitate system has been simulated. A periodic FCC lattice of Er atoms was created. This system is a $3 \times 3 \times 3$ repeat of the FCC cubic cell. In one of the cubic cells, oxygen atoms are placed in 6 of the tetrahedral sites of the Er lattice with the two vacant sites along the $[1\ 1\ 1]$ direction. This structure corresponds to one of the FCC sub-cells of the bixbyite structure. In the remainder of the system, hydrogen atoms are placed in the tetrahedral sites of the erbium lattice consistent with the hydride phase. This models a very small cubic oxide precipitate of 6 oxygen atoms that is about 0.5 nm on a side. Both the atomic positions and the overall volume of the cell were relaxed at zero pressure.

The energy of a He interstitial in this model oxide precipitate is somewhat unexpected. If the He is placed in the center octahedral-like site of the precipitate, O_1 , the energy is 1.19 eV. This is 0.25 eV higher than for the O_1 site in the zero-pressure pure oxide. This increase is consistent with the constraint on the oxide by the surrounding hydride. The surprising result is for interstitial energy of the He in the vacant tetrahedral site, 0.76 eV. This is 0.04 eV lower in energy than for the zero-pressure pure oxide. Examination of the erbium atom locations surrounding this site show that the distance from the center of the site to the surrounding erbium atoms is 0.249 nm which is 0.004 nm greater than the corresponding distance in the pure oxide. This suggests that the local relaxations at the oxide-hydride interface may further favor He trapping, though this effect is rather modest.

The oxide precipitate is also expected to induce strains in the surrounding hydride phase. To assess the magnitude of that effect, the energy of He interstitials in octahedral sites adjacent to the oxide was computed. The computed energies are 1.48, 1.54 and 1.50 eV for He located in adjacent octahedral sites located in the $[1\ 0\ 0]$, $[1\ 1\ 0]$ and $[1\ 1\ 1]$ directions, respectively. These energies are all below the value of 1.64 eV for the He atom in an octahedral site of the ideal hydride. This is consistent with the hydride being locally dilated near the oxide. It also demonstrates that this dilation is directionally dependent. The energetics of the formation of hydrogen vacancies and the energetics of helium located in those vacancies has not yet been determined.

Chapter 4

He diffusion barriers

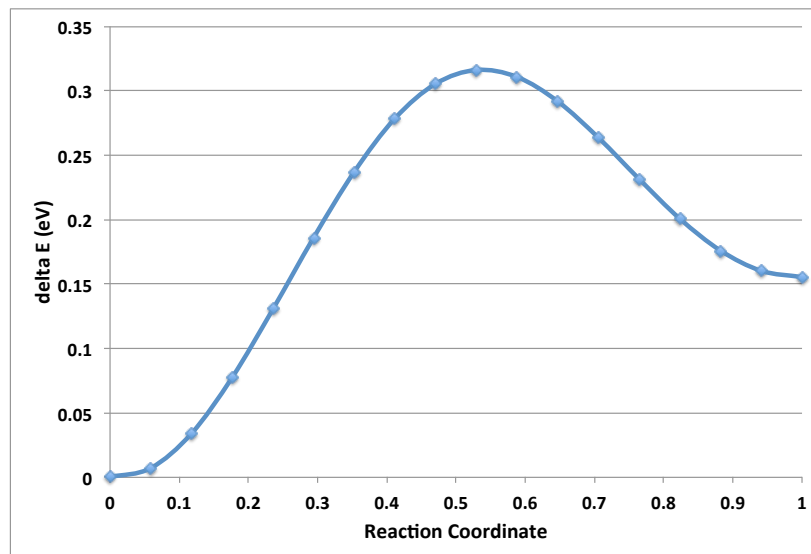
DFT nudged elastic band (NEB) calculations were performed using VASP to determine the migration paths between the available He sites in erbium oxide. First, the transition paths between two T sites were computed. This included the transition not only between two T sites located in the same quasi-FCC unit cell along a diagonal, but also between two nearby T sites located in different diagonal rows. In both cases, it was found that the transition path traverses through the octahedral sites. The motion of the He interstitial between T sites within a quasi-FCC unit cell T sites proceeds by the transition $T \rightarrow O_1$. Once in the O_1 site, the He can either jump back to the original T site or advance to the other T site in the quasi-FCC unit cell.

The other fundamental transition is $T \rightarrow O_2$. In this transition, the He atom jumps from the T site to one of the three O_2 sites located on the cell edges closest to the T site. Once in the O_2 site, the He can either return to its original site or jump to a T site that is located in a different quasi-FCC cell. Note that a detailed examination of the crystal structure shows that the neighboring cell that has a T site close to the O_2 site is the cell that shares a common face with the original cell. Thus the net result is the motion of the He atom from one quasi-FCC unit cell to an adjacent cell that shares a common face.

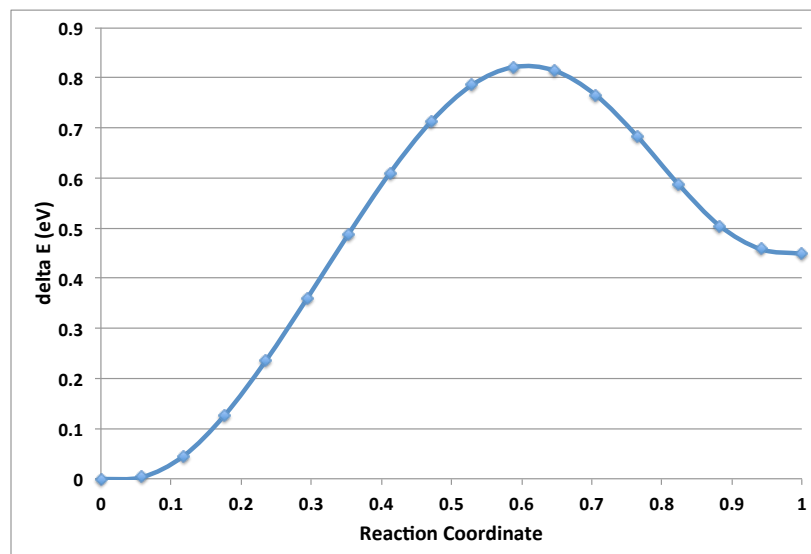
The barriers for these two processes are depicted in Figure 4.1. The energy barrier to jump from T to O_1 is 0.32 eV and the energy barrier to jump from T to O_2 is 0.81 eV. With these barriers, it is expected that a He atom would jump between the two sites in a quasi-fcc cell on a microsecond time scale at room temperature. Jumps between cells would be expected to occur on a time scale of tens of seconds at room temperature.

In order to ascertain whether or not oxide precipitates serve as effective traps for helium, we must examine the barriers to motion across the interface between the hydride and the oxide. Consider an octahedral site in the interface plane. The two crucial barriers are the motion of the He atom from this site into the vacant tetrahedral sites of the oxide and the barrier to reach this interfacial site from an adjacent octahedral site in the hydride. Figure 4.2 shows the computed barriers as a function of the reaction coordinate for these two transitions. This is shown as a continuous transition that starts at the octahedral site of the hydride and ends at the T site of the oxide. The mid-point of this curve corresponds to the He atom at the octahedral-like site in the interface plane. Note that the rate limiting step is the motion of the He atom from the octahedral site in the hydride to the site at the interface plane. From this site the subsequent motion into the T site of the oxide has only

a very small barrier.



(a)



(b)

Figure 4.1. The energy as a function of the reaction coordinate for the motion of the He atom from the T site to the a) O1 site and to the b) O2 site.

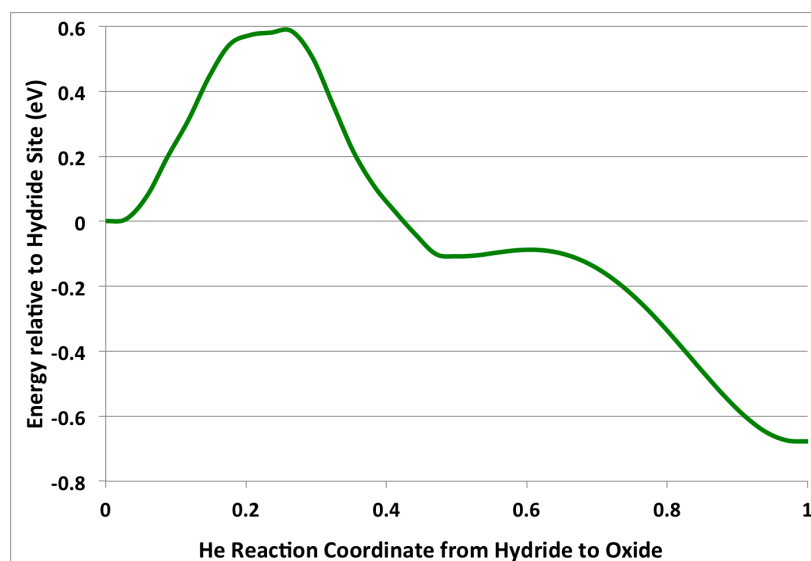


Figure 4.2. The energy along the He transition path from an octahedral site in the hydride adjacent to the oxide through an octahedral site in the interface plane, reaction coordinate = 0.5, to a vacant tetrahedral site in the oxide.

Chapter 5

Kinetic Models

The DFT calculations described in the preceding sections provide the input needed to develop a kinetic Monte Carlo (kMC) model of the diffusion of He in ErH₂ with Er₂O₃ precipitates. A simplified kMC model of the ErH₂ + Er₂O₃ system was constructed by assuming that each unit cell in the crystalline lattice can be represented by a single site in the kMC model. Since we are interested primarily in the interaction between He and Er₂O₃, this approximation is sufficient for the present purposes. A fully atomic model of the system is currently being implemented into Sandia’s SPPARKS software [8].

The model system was created using a simple cubic lattice of 256³ Monte Carlo sites. (Recall that each Monte Carlo site represents a unit cell of the material.) The desired fraction of these unit cells were designated randomly as oxide, and the remainder as hydride. A single helium atom was placed at a random location in the simulation domain, and allowed to diffuse according to rates based on activation energy barriers from DFT calculations. The rate of any diffusive “hop” has the form.

$$r = \exp\left(-\frac{E_b}{kT}\right), \tag{5.1}$$

where r is the rate of the hop, E_b is the energy barrier between the beginning and ending (ground) states of the hop, k is Boltzmann’s constant, and T is the temperature. The energy barrier, and therefore the associated rate, are determined based on the phase (hydride or oxide) that the helium atom is diffusing from and to. These values are shown in Table 5.1. In cases where more than one viable diffusion path is possible, the rates for each path are evaluated individually and then summed to produce the total rate of diffusion for that case. Given this diffusion mechanism, the associated kinetic data - i.e. rates, and the initial conditions described above - a standard kMC algorithm [1, 3, 4, 5] was applied to simulate 10⁹ diffusive events, i.e. Monte Carlo steps, at oxide volume percentages of 0.01%, 0.05%, 0.1%, 0.5%, and 1%, and temperatures ranging from approximately 250 K to 1050 K. The residence times of the diffusing helium atom in the two different phases (hydride and oxide) were calculated, and the results are shown in Fig 5.1. Despite the relatively low oxide concentrations studied here, the helium diffuser spends the majority of its time trapped in the oxide phase, except at the lowest oxide concentrations and highest temperatures.

Table 5.1. Energy barriers for helium diffusion between the hydride and oxide phases of erbium. Multiple values indicate more than one viable diffusion path for that case, for which the associated diffusion rates - see Equ 5.1 - are summed.

From \ To	ErH ₂	Er ₂ O ₃
ErH ₂	0.49 eV, 0.98 eV [14]	0.69 eV
Er ₂ O ₃	1.28 eV	0.32 eV, 0.81 eV

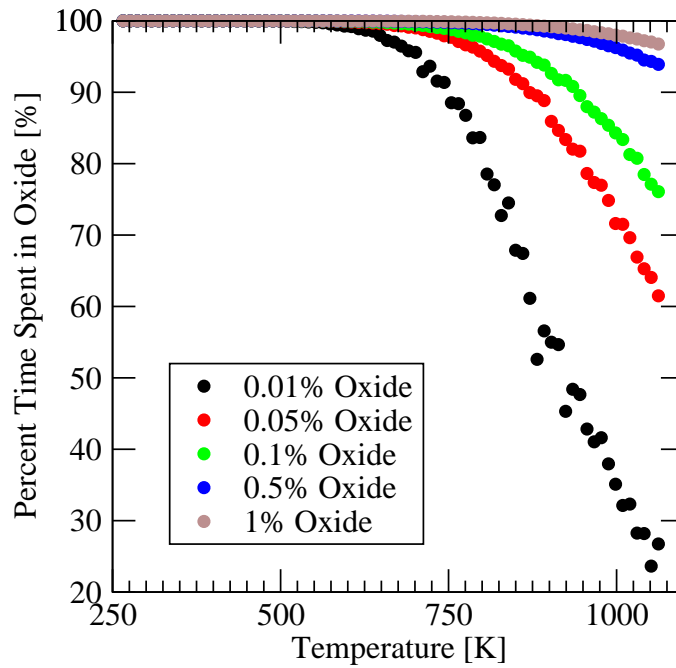


Figure 5.1. The percent of the total simulation time that the diffusing helium atom spends in the oxide phase, as a function of temperature, for several oxide volume fractions.

Chapter 6

Summary

The formation of He bubbles in erbium tritides is a crucial process in the aging of these materials. The detailed mechanisms underlying the nucleation of these bubbles remain a mystery. Thus there is interest in understanding the fundamental processes that lead to the localization of He in erbium hydrides. Previous work did not help identify obvious nucleation sites in homogeneous erbium hydride.

This work builds on the observation that erbium hydrides have nano-scale erbium oxide precipitates due to the high thermodynamic stability of erbium oxide and the ubiquitous presence of oxygen during materials processing. Fundamental DFT calculations indicate that the He is energetically favored in the oxide relative to the bulk hydride. Activation energies for the motion of He in the oxide and at the oxide-hydride interface indicate that trapping is kinetically feasible. A simple kinetic Monte Carlo model is developed that demonstrates the degree of trapping of He as a function of temperature and oxide fraction. The main result of this study is that, in the absence of any other trapping sites, He will accumulate in these oxide precipitates. Thus the oxide may play a role in the initial formation of He bubbles.

While these results point to the potential importance of the oxide precipitates, there are still significant unanswered questions. While the oxides are coherent in the hydride matrix, there is a small lattice constant mismatch. This will produce strain fields that can influence the diffusion of He in the lattice. The presence of additional (as yet unidentified) trap sites could alter the stability of He in the oxide. In particular, the equilibrium between He in the oxide precipitates and He in established He bubbles has not yet been determined. Finally, the process(es) by which He trapped in the oxides might evolve into bubbles is still unknown.

References

- [1] C. C. Battaile. The kinetic monte carlo method: Foundation, implementation, and application. *Computer Methods in Applied Mechanical Engineering*, 192:3386–3398, 2008.
- [2] Y. E. Bogatov, A. K. Molodkin, M. G. Safronenko, and Y. Y. Nevyadomskaya. Re interaction with titanium(iii) oxide. *Russion Journal of Inorganic Chemistry*, 39:223–228, 1994.
- [3] A. B. Bortz, M. H. Kalos, and J. L. Lebowitz. A new algorithm for monte carlo simulation of ising spin systems. *J. Comp. Phys.*, 17:10–18, 1975.
- [4] K. A. Fichthorn and W. H. Weinberg. Theoretical foundations of dynamical monte carlo simulations. *J. Chem. Phys.*, 95:1090–1096, 1991.
- [5] D. T. Gillespie. Exact stochastic simulation of coupled chemical reactions. *J. Phys. Chem.*, 81:2340–2361, 1977.
- [6] G. Kresse and J. Furthmuller. Efficient interactive scheme for ab initio total-energy calculations using a plane-wave basis set. *Physical Review B*, 54(16):11169–11186, 1996.
- [7] G. Kresse and D. Joubert. From ultrasoft pseudopotentials to the projector augmented-wave method. *Physical Review B*, 59:1758–1775, 1999.
- [8] Sandia National Laboratories. Stochastic parallel particle kinetic simulator (spparks). <http://spparks.sandia.gov/>.
- [9] W Mao, T. Chikado, A. Suzuki, T. Terai, and K. Yamaguchi. Experimental and computational studies on tritium permeation mechanism in erbium oxide. *Journal of Plasma and Fusion Research*, 10:27–32, 2013.
- [10] T. B. Massalski, editor. *Binary Alloy Phase Diagrams*, pages 1586–1587. ASM International, 1990.
- [11] H. J. Monkhorst and J. D. Pack. Special points for brillouin-zone integrations. *Physical Review B*, 13(12):5188–5192, 1976.
- [12] C. D. Parish, C. S. Snow, and L. N. Brewer. The manifestation of oxygen contamination in erd2 thin films. *Journal of Materials Research*, 24:1868–1879, 2009.
- [13] C. S. Snow, J. F. Browning, G. M. Bond, M. A. Rodriguez, and J. A. Knapp. ^3He bubble evolution in ErT_2 : A survey of experimental results. *Journal of Nuclear Materials*, 453:296–306, 2014.

- [14] R. R. Wixon, J. F. Browning, C. S. Snow, P. A. Schultz, and D. R. Jennison. First principles site occupation and migration of hydrogen, helium and oxygen in beta-phase erbium hydride. *Journal of Applied Physics*, 103:123708, 2008.

Appendix A

DFT Calculations

The electronic structure calculations are performed using the Vienna Ab Initio Simulation Package (VASP) [6]. This is a plane-wave basis implementation of density functional theory (DFT). These calculations employed the generalized gradient approximation (GGA) with pseudopotentials of the projector-augmented-wave method (PAW) [7]. The pseudopotentials are taken from the VASP library. The numbers of valence electrons treated are 9, 6, 2 and 1 for Er, O, He and H respectively. For calculations involving multiple elements, it is important to use the same energy cut-off for the plane-wave basis. Of the elements considered here, the hardest pseudopotential (the pseudopotential that requires the most extensive plane-wave basis) is He. The energy cut-off required for He is 600 eV and so that plane-wave cut-off is used for all calculations reported here. The k-space integrations are performed using the Monkhorst-Pack integration scheme [11]. The size of the k-space grid depended on the system considered, but in all cases it was determined that energy differences are converged to better than 0.01 eV. The nudged elastic band (NEB) calculations were performed using the algorithm implemented in the VASP code with 16 intermediate configurations.

DISTRIBUTION:

- 1 MS 0899 Technical Library, 9536 (electronic copy)

